

# Microstructural Characterization and Growth Kinetics of the Reaction Layer in U-10wt% Zr/Zircaloy-4 Diffusion Couples

Zhang Yuting<sup>1,2</sup>, Wang Xin<sup>1</sup>, Liu Pengchuang<sup>1</sup>, Zeng Gang<sup>3</sup>, Pang Xiaoxuan<sup>3</sup>,  
Jia Jianping<sup>3</sup>, Sheng Liusi<sup>2</sup>, Zhang Pengcheng<sup>1</sup>

<sup>1</sup> Science and Technology on Surface Physics and Chemistry Laboratory, Jiangyou 621908, China; <sup>2</sup> School of Nuclear Science and Technology, University of Science and Technology of China, Hefei 230029, China; <sup>3</sup> Institute of Materials, China Academy of Engineering Physics, Mianyang 621907, China

**Abstract:** To investigate the compatibility and diffusion behavior between U-Zr alloys and Zr-4 alloys, solid-to-solid U-10wt% Zr/Zr-4 diffusion couples were assembled by vacuum hot pressing and then annealed under vacuum at temperatures ranging from 580 °C to 1100 °C for various time. Scanning and transmission electron microscopes were employed to analyze the microstructures and composition profiles at the interfaces of the couples. The compatibility between the two alloys was investigated.  $\delta$ -UZr<sub>2</sub> and ~20-nm-thin U-rich layers existed in the vacuum-hot-pressed samples. The interdiffusion coefficient constant and activation energy are found to be  $(4.23 \pm 0.63) \times 10^{-6}$  m<sup>2</sup>/s and  $(160.73 \pm 1.67)$  kJ/mol, respectively. The interdiffusion coefficients of the U-10wt% Zr/Zr-4 alloy couples are higher than those of U-Zr alloys, especially at low temperature.

**Key words:** metallic fuel; cladding; interface; interdiffusion; hybrid reactor

Metallic fuels possess high breeding ratio, high burn-up, good thermal conductivity, hard neutron spectrum, high fissile capability and fertile material density, short doubling time, and simplified reprocessing and refabrication, which make them promising candidates for next-generation reactors, such as traveling-wave reactors<sup>[1-3]</sup>, sodium-cooled fast reactors<sup>[4-11]</sup>, and fusion-fission hybrid reactors (FFHRs)<sup>[12-14]</sup>. Metallic fuels have several advantages, such as simple fabrication, inherent safety characteristics<sup>[6]</sup>, a favorable thermal response<sup>[4]</sup>, and relatively easy recycling using compact pyroprocessing treatment. Uranium-zirconium alloys are considered promising metallic fuels. The addition of zirconium to uranium increases the melting point, enhances the corrosion resistance, reduces fuel-cladding chemical interaction (FCCI), and improves the dimensional stability under irradiation<sup>[8, 11, 15-18]</sup>. To reduce the interactions between a U-Zr fuel and a cladding, pure Zr foil has been suggested as a diffusion barrier between

U-Zr alloys and steel cladding<sup>[19-21]</sup> to eliminate FCCI, which is considered to be a potential problem in the application of metallic fuels in fast reactors. The addition of trace elements such as Sn, Nb, and Fe to pure zirconium enhances its corrosion resistance. These Zr alloys have been extensively used as cladding materials in light water reactors (LWRs)<sup>[22]</sup>. Because of the above advantages, Lightbridge Corporation is developing an advanced metallic nuclear fuel clad in Zr alloy to increase the power output and extend the cycle length of current LWRs<sup>[13, 23]</sup>. China is investigating the use of Zircaloy-4 (Zr-4) as a cladding material for U-10wt% Zr alloy fuels in FFHRs<sup>[12]</sup>.

U-Zr alloys can act as a nuclear fuel for next-generation reactors. The fabrication method of the fuel rod plays a role in determining whether it behaves well in the relevant nuclear fuel cycle. A U-Zr fuel and Zr-Nb cladding has been extruded or hot-rolled to assemble fuel rods<sup>[24, 25]</sup>, however, mechanical working may introduce texture into the materials. Furthermore,

Received date: September 10, 2017

Foundation item: National Natural Science Foundation of China (91226203); ITER (2012GB106004)

Corresponding author: Zhang Yuting, Ph. D., Science and Technology on Surface Physics and Chemistry Laboratory, Jiangyou 621908, P. R. China, Tel: 0086-816-3626738, E-mail: zhangyuting@caep.cn

Copyright © 2018, Northwest Institute for Nonferrous Metal Research. Published by Elsevier BV. All rights reserved.

the diffusion data and compatibility between the U-Zr alloy fuel and cladding are important for understanding the post-irradiation behavior of fuel rods. Uranium diffusion in pure zirconium was examined experimentally to obtain diffusion data in the temperature ranges of 540–850 °C<sup>[25]</sup> and 915–1200 °C<sup>[26]</sup>. Pure zirconium metal foils were effective in inhibiting interdiffusion between the U-Zr alloy fuel and a steel cladding<sup>[19, 27]</sup>. Interdiffusion between U-Zr alloys and Zr alloys differs slightly from that in U/Zr couples because the interdiffusion coefficients in uranium depend on the Zr content of U-Zr alloys and minor elements added into zirconium alloy. Although very limited data on diffusion between U-Zr alloys and Zr alloys are available, there are several studies on the compatibility between a U-Mo alloy and pure Zr under the Reduced Enrichment for Research and Test Reactor Program<sup>[28-30]</sup>. Gordillo et al.<sup>[25]</sup> reported the interdiffusion behavior of U-10wt% Zr/ Zr-4 at elevated temperatures of 700–800 °C for a short time and extrapolated the diffusion data. To systematically investigate the compatibility of the U-10wt% Zr alloy and Zr-4 alloy, it is necessary to investigate the phase constituents and microstructure that develop during fuel rod fabrication and the interdiffusion between U-10wt% Zr and Zr-4 at various temperatures for a longer time.

This study examined the phase constituents and microstructure of fuel rod assemblies after vacuum hot pressing (VHP) with high-temperature annealing. Scanning electron microscopy (SEM) and transmission electron microscopy (TEM) with X-ray energy-dispersive spectroscopy (EDS) were adopted to observe the phase constituents and microstructure between the U-10wt% Zr fuel and Zr-4 cladding. Concentration profiles were determined by SEM-EDS to study the growth kinetics of phases at the interfaces and the interdiffusion behavior between the fuel and cladding.

## 1 Experiment

The U-10wt% Zr alloy employed in this investigation was cast by induction melting with high-purity depleted uranium and 99.95% pure zirconium. The alloys were flipped and remelted three times to ensure homogeneity and were then drop-cast to form rods. The Zr-4 rods were acquired from a commercial source; the chemical composition of Zr-4 is given in Table 1.

Both the U-10wt% Zr and Zr-4 rods were sectioned into discs with 12.5 mm in diameter and 2 mm in thickness. The surfaces of the discs were metallographically polished to 1 μm using alumina paste; both faces of the discs were flat, and they were parallel to each other. Then, to remove the residual oxide scale, the Zr-4 was acid-washed for 2 s using a mixture of 45% nitric acid, 10% hydrofluoric acid, and 45% deionized

water. Next, etched Zr-4 discs were washed in deionized water to remove F<sup>-</sup> ions. After a set of wet mechanical polishing treatments and washing, the discs of U-10wt% Zr and Zr-4 were ultrasonicated sequentially in acetone and ethanol for 5 min each to remove the oil and other impurities on the surface.

All of the U-10wt% Zr/Zr-4 couples annealed under vacuum were prepared by VHP bonding. The polished and cleaned discs of U-10wt% Zr and Zr-4 alloys were stacked face-to-face in contact with each other in a VHP furnace with a pressure of  $<5 \times 10^{-3}$  Pa. To ensure adhesion between the U-10wt% Zr and Zr-4, VHP bonding used both heat and pressure to form solid-state bonds between the fuel and cladding. VHP bonding was performed at 580 °C and 200 MPa for 2 or 8 h. To evaluate the effect of VHP bonding on the interfacial microstructure of the couples, the diffusion and reaction behaviors were studied in U-10wt% Zr/Zr-4 couples prepared by VHP bonding before annealing for various time.

To study the growth kinetics of the reaction layer in the U-10wt% Zr/Zr-4 diffusion couples, each couple was VHP bonded at 580 °C and 200 MPa for 2 h and then encapsulated in a quartz capsule that was sealed under vacuum ( $5 \times 10^{-6}$  Pa). Next, the couples were annealed using a tubular furnace at temperatures of 580–1100 °C for various time. After annealing, the diffusion couples were quenched by breaking the quartz capsule in cold water.

Each diffusion couple was cross-sectioned, mounted in epoxy, and metallographically polished to 0.25 μm for microstructural examination and compositional analysis.

The surface of each diffusion couple was examined by focused ion beam (FIB)/SEM (FEI Helios 650 dual beam/scanning electron microscope). For each couple, SEM analysis was conducted to examine the microstructure. To measure the thickness of the interaction zone (IZ), EDS was employed to obtain the concentration profiles of U and Zr by a line scan with a 0.5 μm step size and an accelerating voltage of 20 kV. To determine the average thickness of the IZ developed by interdiffusion during annealing and its standard deviation, the data were measured at 12 randomly selected locations for each diffusion couple. For the diffusion couple bonded by VHP at 580 °C and 200 MPa for 8 h, TEM samples were prepared using an FIB in-situ lift-out technique. Selected area diffraction (SAED), EDS, and high-angle annular dark-field (HAADF) analysis, in combination with the U-Zr phase diagram<sup>[31]</sup>, were used to examine the interdiffusion and reactions between the U-10wt% Zr and Zr-4 alloys.

## 2 Results and Discussion

### 2.1 Interface between U-10wt% Zr and Zr-4 after VHP

Fig.1 shows cross-sectional SEM images and concentration profiles of U-10wt% Zr/Zr-4 diffusion couples vacuum hot pressed at 580 °C for 2 and 8 h. The interdiffusion zone after VHP treatment at 580 °C and 200 MPa for 2 h was narrow (~1.6 μm); the thickness of the diffusion zone was within the experimental

**Table 1 Chemical composition of Zircaloy-4 (wt%)**

Sn	Fe	Cr	C	N	Zr
1.3~1.4	0.2~0.22	0.1~0.12	0.01~0.012	0.006~0.007	Balance

error owing to the limits of the SEM-EDS resolution. As time passed, a discontinuous  $UZr_2$  layer with a width of  $\sim 2.1 \mu m$  was observed in the interface of the U-10wt% Zr/Zr-4 couple VHP-treated at  $580^\circ C$  and 200 MPa for 8 h, as shown in Fig. 1b.

Fig.2 shows a cross-sectional TEM bright image of the  $UZr_2$ /Zr-4 interface in the U-10wt% Zr/Zr-4 diffusion couples vacuum hot pressed at  $580^\circ C$  and 200 MPa for 8 h. The contrast of the interface in Fig.2 indicates that the interface is clean and sharp. The composition profiles drop abruptly as the scanned beam crosses the interface, as shown in Fig.3b. Fig.3a presents a HAADF scanning micrograph of the region between the Zr-4 alloy and  $UZr_2$  layer, where an approximately 20-nm-thick layer of a U-rich phase was observed. The phase constituents could not be identified via SAED analysis

and high-resolution TEM because the U-rich layer was too narrow and the TEM sample was too thick. The U segregation at the  $UZr_2$ /Zr-4 interface is explained by interface free energy minimization<sup>[32, 33]</sup>. U has poor solubility in the Zr-4 alloy at room temperature. Consequently, U atoms will be ejected into the Zr-4 alloy during the growth of  $UZr_2$ . A schematic summary of the interaction layer between the U-10wt% Zr alloy and Zr-4 cladding is presented in Fig.4.

The pre-treatment (VHP at  $580^\circ C$  and 200 MPa for 2 h) could produce U-10wt% Zr/Zr-4 diffusion couples with good bonding that exhibit no cracks or porosity. Therefore, the preparation method of the couples has a negligible impact on the investigation of the interaction between the U-10wt% Zr and Zr-4 alloys.

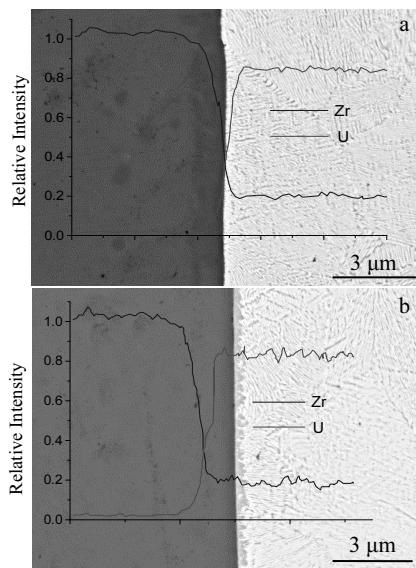


Fig.1 Secondary electron micrographs and Zr, U concentration profiles of U-10wt%Zr/Zr-4 diffusion couples vacuum hot pressed at  $580^\circ C$  for 2 h (a) and 8 h (b)

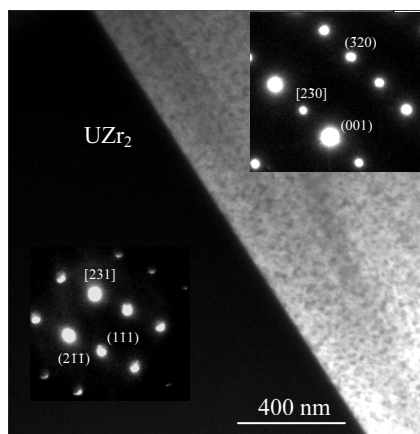


Fig.2 TEM bright-field micrograph of the  $UZr_2$ /Zr-4 interface in the U-10wt% Zr/Zr-4 diffusion couples by vacuum hot pressed at  $580^\circ C$  for 8 h (inset shows the SAED patterns of  $UZr_2$  and Zr-4 alloy)

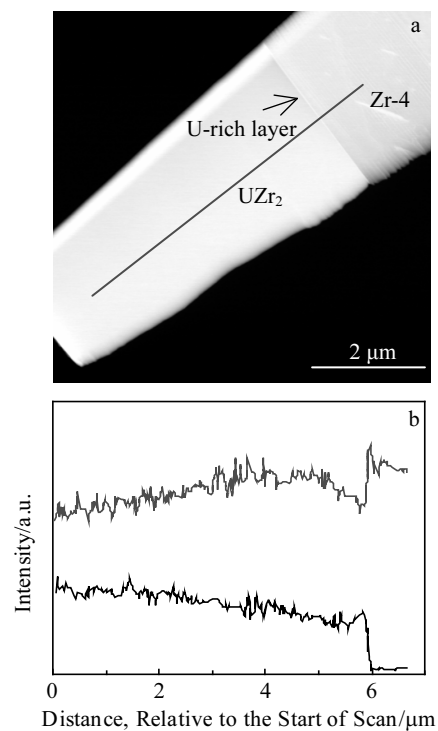


Fig.3 HAADF-STEM micrograph (a) of the  $UZr_2$ /Zr-4 interface in the U-10wt% Zr/Zr-4 diffusion couples vacuum hot pressed at  $580^\circ C$  for 8 h and concentration profile (b) obtained by line scanning along the red line in Fig.3a

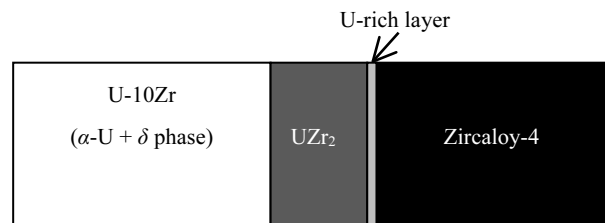


Fig.4 Schematic representing the phase constituents and microstructure of the interaction layers in the U-10wt%Zr/Zr-4 diffusion couples by vacuum hot pressed at  $580^\circ C$  for 8 h

## 2.2 Growth kinetics of the reaction layer in diffusion couples

To study the growth kinetics of the reaction layer between the U-10wt% Zr and Zr-4 alloys, diffusion couples were prepared by VHP at 580 °C and 200 MPa for 2 h and then vacuum-annealed at elevated temperature for various durations. Fig.5 shows typical secondary electron (SE) micrographs and the U and Zr concentration profiles of U-10wt% Zr/Zr-4 couples prepared by VHP and annealed at temperatures of 600–1100 °C for various time. Zr-rich particles (darker areas) were observed on the U-Zr side of the diffusion couples. A continuous intermediate phase of  $\text{UZr}_2$  formed at the interface. The thickness of the diffusion layers at the interface increased with increasing heat-treatment time at these temperatures. The SE images in Fig.5c and 5d show obvious interfaces between the  $\text{UZr}_2$  layers and Zr-4 alloys, and it is difficult to identify the exact location of the  $\text{UZr}_2/\text{U-10wt% Zr}$  interfaces.

To analyze the growth kinetics of the diffusional interaction between the U-10wt% Zr fuel and Zr-4 cladding, the thickness of the IZ was measured from the terminal ends of the U-10wt% Zr and Zr-4 alloys, where the concentration gradient becomes negligible. Table 2 reports the average thickness of

the IZ as a function of the annealing temperature. The numerical data on the thickness of the IZ were measured at 12 randomly selected locations on the EDS line scan for each sample. The interdiffusion coefficient of the U-10wt% Zr/Zr-4 IZ was calculated for annealing at 580, 600, 650, 700, 750, 800, 900, 950, 1000, and 1100 °C, as listed in Table 2 and presented in Fig.6. The principal alloying elements in Zr-4 are Sn, Fe, and Cr, as shown in Table 1. The maximum solubility of Sn in  $\alpha\text{-Zr}$  is about 9.3 wt%, whereas the solubility of Fe in  $\alpha\text{-Zr}$  is very low (120  $\mu\text{g/g}$  at 820 °C<sup>[34]</sup>). Almost all of the Fe would be precipitated as the  $\text{Zr(Fe, Cr)}_2$  type with a Fe/Cr ratio close to 1.5<sup>[35]</sup>, and the solubility of Cr in  $\alpha\text{-Zr}$  is very low. Further, Sn generally remains in solid solution in the hexagonal Zr phase. According to the U-Sn phase diagram, however, when uranium encounters tin, they react to form intermetallics. In addition, considering that the Sn concentration in the Zr-4 alloy is only ~1 at%, the multicomponent alloy system of U-10wt% Zr and Zr-4 was simplified to the U-Zr binary system. Assuming that the growth of the IZ was controlled by diffusion and followed a parabolic growth law<sup>[30]</sup>, the correlation between the thickness and annealing time is expressed as

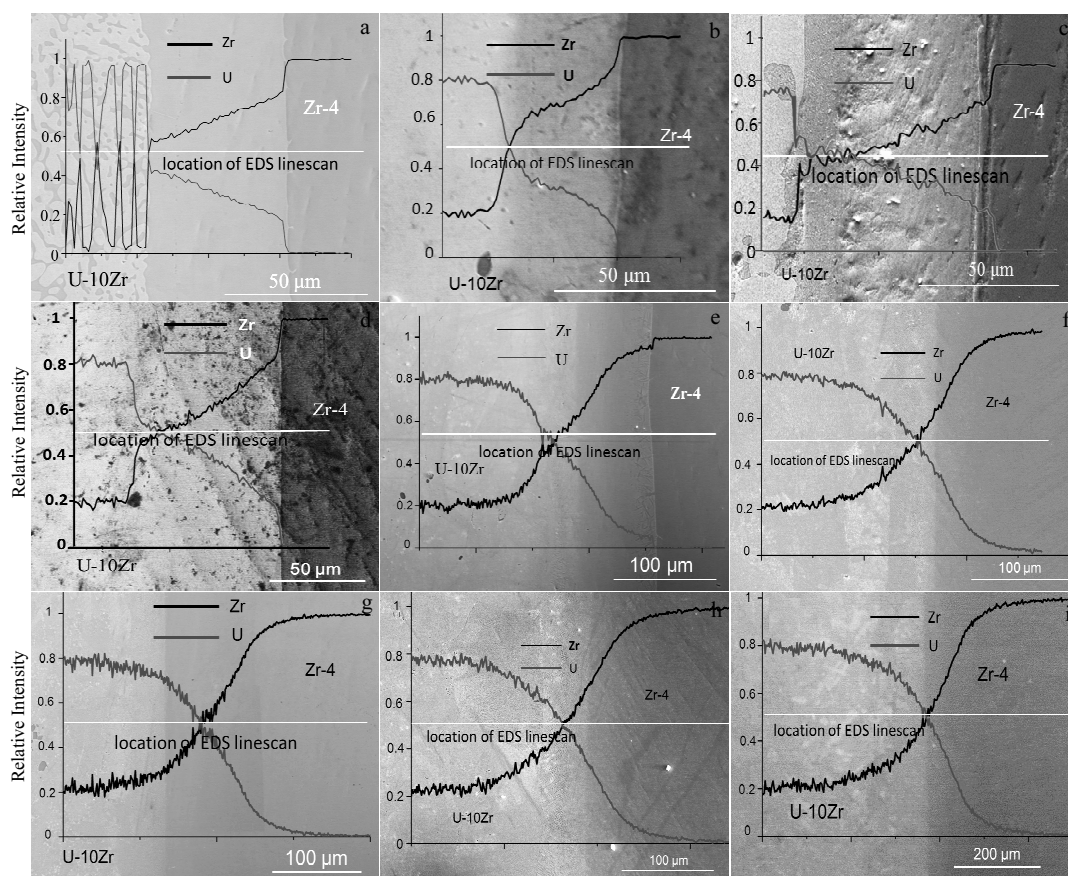


Fig.5 SE micrographs and Zr, U concentration profiles of the water-quenched U-10wt% Zr/Zr-4 diffusion couples annealed at different temperatures and for different time: (a) 600 °C, 192 h, (b) 650 °C, 192 h, (c) 700 °C, 192 h, (d) 750 °C, 192 h, (e) 800 °C, 72 h, (f) 900 °C, 24 h, (g) 950 °C, 24 h, (h) 1000 °C, 12 h, and (i) 1100 °C, 12 h

**Table 2 Interdiffusion coefficients of the interaction zone (IZ) of water-quenched U-10wt% Zr/Zr-4 diffusion couples from this research**

Temperature/°C	Thickness of IZ/ $\mu\text{m}$	Annealing time/h	Diffusion Coefficient, $k/\text{m}^2\cdot\text{s}^{-1}$	Diffusion coefficient constant, $k_0/\text{m}^2\cdot\text{s}^{-1}$	Diffusion activation energy, $Q/\text{kJ}\cdot\text{mol}^{-1}$
1100	528.7±23.4	12	$(3.2\pm 0.3)\times 10^{-12}$		
1000	307.6±23.8	12	$(1.1\pm 0.2)\times 10^{-12}$		
950	312.4±23.5	24	$(5.7\pm 0.9)\times 10^{-13}$		
900	220.0±9.7	24	$(2.8\pm 0.2)\times 10^{-13}$		
800	138.9±10.0	72	$(3.7\pm 0.5)\times 10^{-14}$	$(4.23\pm 0.63)\times 10^{-6}$	$(160.73\pm 1.67)$
750	81.0±4.2	192	$(4.7\pm 0.5)\times 10^{-15}$		
700	67.6±3.5	192	$(3.3\pm 0.3)\times 10^{-15}$		
650	41.0±2.0	192	$(1.2\pm 0.1)\times 10^{-15}$		
600	49.6±2.8	868	$(3.9\pm 0.4)\times 10^{-16}$		
580	13.6±0.7	192	$(1.4\pm 0.2)\times 10^{-16}$		

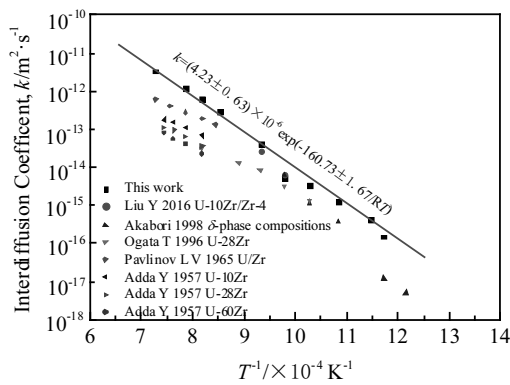


Fig.6 Comparison of the interdiffusion coefficients from this work with those found in the published literature and plot of the calculated values of the diffusivity and activation energy

$$k = x^2/2t \quad (1)$$

where  $k$  is the interdiffusion coefficient,  $x$  is the measured thickness of the IZ, and  $t$  is the annealing time. If the relationship between the diffusion coefficient and temperature obey the Arrhenius relationship, the activation energy for the growth of the IZ is predicted using the relation

$$k = k_0 \exp(-Q/RT) \quad (2)$$

where  $k_0$  is the interdiffusion coefficient constant,  $Q$  is the activation energy,  $R$  is the ideal gas constant, and  $T$  is the annealing temperature in Kelvins. The temperature dependence of  $k$  presented in Fig.6 follows Arrhenius behavior. The interdiffusion coefficient constant and activation energy are  $(4.23\pm 0.63)\times 10^{-6} \text{ m}^2/\text{s}$  and  $(160.73\pm 1.67) \text{ kJ/mol}$ , respectively. The interdiffusion coefficients estimated from the thicknesses of the IZs are considered to represent the interdiffusion coefficient averaged over the Zr concentration range from 10 wt% to near 100 wt%. In Fig.6, these estimated values are compared with the reported interdiffusion coefficients, which are given at various Zr concentrations and temperatures. According to the temperature and the U-Zr system, the data can be divided into four categories.

First, at 900~1100 °C, elements diffuse more rapidly at the

U-10wt% Zr/Zr-4 alloy interface than they do at the U/Zr<sup>[26]</sup> and U-10wt% Zr alloy<sup>[36]</sup> interfaces. Further, the interdiffusion coefficients of U-Zr alloys decrease as the Zr content (above 10 wt%) increases<sup>[36, 37]</sup>. Hence, the interdiffusion coefficient of the IZs in the U-10wt% Zr/Zr-4 alloys is larger than that of the IZs in U-Zr alloys with Zr contents ranging from 10 wt% to near 100 wt%.

Second, at 750~800 °C, the interfaces consist of a  $\gamma$ -U solution and  $\alpha$ -Zr, and the interdiffusion coefficients  $k$  are in good agreement with those reported for U-10wt%Zr/Zr-4 alloys by Gordillo et al<sup>[25]</sup>. Between 750 and 800 °C, the interdiffusion coefficients  $k$  of U-10wt% Zr/Zr-4 alloys were greater than that of U-28wt% Zr alloy, which has the largest interdiffusion coefficient among U-Zr alloys with a Zr content more than 10 wt%<sup>[37]</sup>. Therefore, compared with U-Zr alloys with a Zr content above 10 wt%, elements diffuse more rapidly at the interface between the U-10wt% Zr and Zr-4 alloys.

Third, at 650~750 °C, the interfaces consist of  $\beta$ -U, a bcc( $\gamma$ -U,  $\beta$ -Zr) solid solution, and  $\alpha$ -Zr, where the bcc( $\gamma$ -U,  $\beta$ -Zr) solid solution layers have  $\delta$ -UZr<sub>2</sub> phase compositions, as shown in Fig.5b and 5c.

Finally, at 580~600 °C, the  $\delta$ -UZr<sub>2</sub> phase of the U-Zr system can be expected to form at the interface of the U-10wt% Zr/Zr-4 alloy couples, and the interdiffusion zones of the U-10wt% Zr/Zr-4 alloys consist of  $\alpha$ -U,  $\delta$ -UZr<sub>2</sub>, and  $\alpha$ -Zr. The width of the interdiffusion zone equals that of the bcc ( $\gamma$ -U,  $\beta$ -Zr) solid solution or  $\delta$ -UZr<sub>2</sub> layer. Akabari et al.<sup>[38]</sup> reported the interdiffusion in the U-Zr system with the  $\delta$ -UZr<sub>2</sub> phase composition by applying the Boltzmann–Matano method. In addition, the interdiffusion coefficient  $k$  of U-Zr alloys at these compositions tends to increase slightly with increasing Zr concentration.

Therefore, the interdiffusion coefficients of the U-10wt% Zr/Zr-4 alloy diffusion couples can be compared with the reported data for U-Zr alloys with  $\delta$ -UZr<sub>2</sub> phase compositions<sup>[39]</sup>. The interdiffusion coefficients of the U-10wt% Zr/Zr-4 couples are 2.6, 2.75, and 3.2 times larger than that of U-Zr alloys at 750, 700, and 650 °C, respectively<sup>[37, 38]</sup>. The interdiffusion coefficient  $k$  of the U-10wt% Zr/Zr-4 couples is much larger

than that of the  $\delta$ -UZr<sub>2</sub> phase at 580 °C<sup>[38]</sup>. As the temperature decreased, the difference in the interdiffusion of the above two systems became more obvious. This phenomenon can be explained as follows.

The mechanisms of atomic diffusion in substitutional-type solids are closely connected with defects such as vacancies or interstitials and dislocations<sup>[39]</sup>. The phase boundaries of the Zr matrix and Zr(Fe, Cr)<sub>2</sub> intermetallics can act as high-diffusivity paths because the mobility of atoms is usually much higher along phase boundaries than in the lattice. At low temperature, the interdiffusion coefficient in the  $\delta$ -UZr<sub>2</sub> phase is significantly smaller than that extrapolated from the ( $\gamma$ -U,  $\beta$ -Zr) solid solutions<sup>[38]</sup>. The phase boundaries of Zr(Fe,Cr)<sub>2</sub>/ $\delta$ -UZr<sub>2</sub> and U<sub>3</sub>Sn<sub>2</sub>/ $\delta$ -UZr<sub>2</sub> offer short-circuit diffusion paths. Further, the effects of improving the interdiffusion coefficient are obvious. In the temperature range of 650 to 750 °C, U–Zr systems consist of ( $\gamma$ -U,  $\beta$ -Zr) solid solutions and  $\alpha$ -U or  $\beta$ -U, and the solids have more vacancies; thus, atoms diffuse much more rapidly. As the temperature increases, the ratio of short-circuit diffusion to interdiffusion of U-10wt% Zr/Zr-4 alloy couples becomes smaller.

### 3 Conclusions

1) The interdiffusion coefficient constant and activation energy of U-10wt% Zr/Zr-4 diffusion couples are  $(4.23 \pm 0.63) \times 10^{-6} \text{ m}^2/\text{s}$  and  $(160.73 \pm 1.67) \text{ kJ/mol}$ , respectively.

2) Compared with those of U-Zr alloys, the interdiffusion coefficients of the U-10wt% Zr/Zr-4 couples are larger below 750 °C, which is attributed to phase boundaries between dispersed intermetallics and the matrix.

### References

- 1 Terra Power L. *Proceeding of ICAPP*[C]. Illinois: American Nuclear Society, 2010
- 2 Hejzlar P, Petroski R, Cheatham J et al. *Nuclear Engineering and Technology*[J], 2013, 45(6): 731
- 3 Hartanto D, Heo W, Kim C et al. *Nuclear Engineering and Technology*[J], 2016, 48(2): 330
- 4 Carmack W, Porter D, Chang Y et al. *Journal of Nuclear Materials*[J], 2009, 392(2): 139
- 5 Burkes D E, Fielding R S, Porter D L et al. *Journal of Nuclear Materials*[J], 2009, 389(3): 458
- 6 Sofu T. *Nuclear Engineering and Technology*[J], 2015, 47(3): 227
- 7 Burkes D E, Fielding R S, Porter D L. *Journal of Nuclear Materials*[J], 2009, 392(2): 158
- 8 Hofman G L, Walters L C, Bauer T. *Progress in Nuclear Energy*[J], 1997, 31(1): 83
- 9 Mcfarlane H F, Lineberry M J. *Progress in Nuclear Energy*[J], 1997, 31(1-2): 155
- 10 Till C, Chang Y, Hannum W. *Progress in Nuclear Energy*[J], 1997, 31(1-2): 3
- 11 Walters L. *Journal of Nuclear Materials*[J], 1999, 270(1): 39
- 12 Li Maosheng, Liu Rong, Shi Xueming et al. *Fusion Engineering and Design*[J], 2012, 87(7): 1420
- 13 Malone J, Totemeier A, Shapiro N et al. *Nuclear Technology*[J], 2012, 180(3): 437
- 14 Wu Hongchun, Zu Tiejun, Qiu Suisheng et al. *Progress in Nuclear Energy*[J], 2013, 64: 1
- 15 Walter C, Golden G, Olson N. Report ANL-76-28[R]. Illinois: Argonne National Laboratory, 1975
- 16 Pahl R, Porter D, Lahm C et al. *Metallurgical Transactions A*[J], 1990, 21(7): 1863
- 17 Bullock J. *Physical Metallurgy of Uranium Alloys*[M] Chicago: Brook Hill, 1976
- 18 Hilton B A. ANL 00/24[R]. Illinois: Argonne National Laboratory, 2000: 75
- 19 Ryu H J, Lee B O, Oh S J et al. *Journal of Nuclear Materials*[J], 2009, 392(2): 206
- 20 Kim J H, Ryu H J, Baek J H et al. *Journal of Nuclear Materials*[J], 2009, 394(2): 144
- 21 Keiser Jr D D, Cole J I. *Global 2007 Conference on Advanced Nuclear Fuel Cycles and Systems*[C]. Illinois: American Nuclear Society, 2007: 109
- 22 He L, Harp J M, Hoggan R E et al. *Journal of Nuclear Materials*[J], 2017, 486: 274
- 23 Malone J, Totemeier A, Morozov A. *Transactions of the American Nuclear Society*[J], 2011, 104: 729
- 24 Lee C T, Park J H, Kim T K et al. *Journal of Nuclear Materials*[J], 2008, 373(1): 275
- 25 Gordillo J A, Perz R A, Iribarren M et al. *Journal of Nuclear Materials*[J], 2015, 462: 85
- 26 Pavlinov L V, Nakonechnikov A I, Bykov V N. *Atomic Energy*[J], 1965, 19: 1495
- 27 Keiser D D. *Defect and Diffusion Forum*[C]. Zürich: Trans Tech Publications, 2007: 131
- 28 Perez E, Yao B, Keiser J R D et al. *Journal of Nuclear Materials*[J], 2010, 402(1): 8
- 29 Jue J F, Keiser D D, Breckenridge C R et al. *Journal of Nuclear Materials*[J], 2014, 448: 250
- 30 Park Y, Yoo J, Huang K et al. *Journal of Nuclear Materials*[J], 2014, 447: 215
- 31 Sheldon R, Peterson D. *Bulletin of Alloy Phase Diagrams*[J], 1989, 10(2): 165
- 32 Marquis E A, Seidman D N, Asta M et al. *Acta Materialia*[J], 2006, 54(1): 119
- 33 Kang S J, Kim Y W, Kim M et al. *Acta Materialia*[J], 2014, 81: 501
- 34 Charquet D, Hahn R, Ortlieb E et al. *Zirconium in the Nuclear Industry: Eighth International Symposium*[C]. Pennsylvania: ASTM International, 1989: 405
- 35 Toffolon-Masclat C, Branchet J C, Jago G. *Journal of Nuclear Materials*[J], 2002, 305(2): 224
- 36 Fedorov G B, Smirnov E A, Zhomov F I et al. *Atomic Energy*[J], 1971, 31: 1280
- 37 Ogata T, Akabori M, Itoh A et al. *Journal of Nuclear Materi-*

- als[J], 1996, 232: 125
- 38 Akabori M, Itoh A, Ogawa T et al. *Journal of Alloys and Compounds*[J], 1998, 271: 597
- 39 Mehrer H. *Diffusion in Solids: Fundamentals, Methods, Materials, Diffusion-Controlled Processes*[M]. Springer Science & Business Media, 2007

## U-10Zr/Zr-4 合金界面的微观结构及生长动力学研究

张羽廷<sup>1,2</sup>, 王 鑫<sup>1</sup>, 刘朋闯<sup>1</sup>, 曾 钢<sup>3</sup>, 庞晓轩<sup>3</sup>, 贾建平<sup>3</sup>, 盛六四<sup>2</sup>, 张鹏程<sup>1</sup>

(1. 表面物理与化学重点实验室, 四川 江油 621908)

(2. 中国科学技术大学 核科学技术学院, 安徽 合肥 230029)

(3. 中国工程物理研究院 材料研究所, 四川 绵阳 621907)

**摘要:** 为研究 U-Zr 合金与 Zr-4 合金之间的相容性和扩散行为, 采用真空热压扩散法制备 U-10wt%Zr/Zr-4 扩散偶, 随后在高真空中 580~1100 °C 高温热处理样品。采用扫描电镜和透射电镜分析检测扩散偶的界面微观结构和元素分布。系统研究了两种合金之间的相容性。 $\delta$ -UZr<sub>2</sub> 层和厚约 20 nm 的富铀层形成于热压扩散法制备的样品界面。测量了合金界面扩散系数常数和扩散激活能, 分别为  $(4.23 \pm 0.63) \times 10^{-6} \text{ m}^2/\text{s}$  和  $(160.73 \pm 1.67) \text{ kJ/mol}$ 。结果表明 U-10wt%Zr/Zr-4 扩散偶的扩散系数大于 U-Zr 合金的, 特别是在低温段。

**关键词:** 金属型核燃料; 包壳; 界面; 互扩散; 混合堆

---

作者简介: 张羽廷, 男, 1983 年生, 博士, 高级工程师, 表面物理与化学重点实验室, 四川 江油 621908, 电话: 0816-3626738, E-mail: zhangyuting@caep.cn